

LASER BIOLOGY

PACS numbers: 42.25.Ja, 42.25.Lc, 47.63.Jd, 42.25.Fx, 42.25.Kb, 42.30.Wb
DOI: 10.1070/QE2011v041n02ABEH014215

Laser diagnostics of anisotropy in birefringent networks of biological tissues in different physiological conditions

Yu.A. Ushenko, Yu.Ya. Tomka, A.V. Dubolazov

Abstract. **We study the possibility of differentiation of optical anisotropy properties of biological tissues in different physiological conditions by means of statistical analysis of coordinate distributions of a new analytic parameter, namely, the complex degree of mutual anisotropy of extracellular matrix, formed by a network of birefringent filament-like protein crystals.**

Keywords: *polarisation, birefringence, correlation, biological tissue, statistics.*

1. Introduction

The laser methods for studying the structure of biological tissues (BTs) are traditionally divided into three groups:

(i) spectrophotometric methods [1–3], based on the analysis of spatial or temporal variations in the intensity of laser radiation, scattered by the BT;

(ii) polarisation methods, based on the use of the complex amplitude coherence matrix [4,5] and the analysis of the degree of polarisation as a correlation factor for complex orthogonal components of electromagnetic oscillations in one of the points of the scattered laser radiation field [3,6–21];

(iii) correlation methods, based on the analysis of the degree of correlation of parallel polarisation components of optical vibrations in different points of the object field [7,21–26].

In [5,22,26–31] a new approach is proposed for the complex analysis of polarisation-inhomogeneous laser radiation fields, based on the generalisation of the coherence matrix $\{K(r,\tau)\}$, namely, the polarisation coherence matrix $\{\Phi(r_1,r_2,\tau)\}$ for two points (r_1,r_2):

$$\{K(r,\tau)\} \to \{\Phi(r_1,r_2,\tau)\}. \tag{1}$$

In the detailed form (1) may be rewritten in the form:

$$\begin{Vmatrix} \langle U_x(r,\tau)U_x^*(r,\tau)\rangle & \langle U_x(r,\tau)U_y^*(r,\tau)\rangle \\ \langle U_y(r,\tau)U_x^*(r,\tau)\rangle & \langle U_y(r,\tau)U_y^*(r,\tau)\rangle \end{Vmatrix} \to \begin{Vmatrix} \langle U_x(r_1,\tau)U_x^*(r_2,\tau)\rangle & \langle U_x(r_1,\tau)U_y^*(r_2,\tau)\rangle \\ \langle U_y(r_1,\tau)U_x^*(r_2,\tau)\rangle & \langle U_y(r_1,\tau)U_y^*(r_2,\tau)\rangle \end{Vmatrix}. \tag{2}$$

Yu.A. Ushenko, Yu.Ya. Tomka, A.V. Dubolazov Yuriy Fedkovych Chernivtsi National University, ul. Kotsubinsky 2, 58012 Chernivtsi, Ukraine, e-mail: yuriyu@gmail.com

Received 13September 2009; revision received 19 November 2010
Kvantovaya Elektronika **41** (2) 170–175 (2011)
Translated by V.L. Derbov

Here, the angle brackets denote the operation of averaging over the time τ of the orthogonal components U_x, U_y of the electromagnetic wave complex amplitude at the points with the coordinates (r_1,r_2).

In [23] the coordination between the object field polarisation states at the points r_1, r_2 with the intensities $I(r_1,\tau)$ and $I(r_2,\tau)$ is characterised by means of a new parameter, namely, the complex degree of mutual polarisation (CDMP) $V(r_1,r_2,\tau)$ having the analytic form:

$$V(r_1,r_2,\tau) = 4\frac{\nu_1^2+\nu_2^2+\nu_3^2}{I(r_1,\tau)I(r_2,\tau)}, \tag{3}$$

where the coefficients ν_i are defined as intensity differences of interference patterns, formed by the electromagnetic waves, travelling from the points r_1, r_2:

$$\nu_1 = \frac{\langle U_x(r_1,\tau)U_x^*(r_2,\tau)\rangle - \langle U_y(r_1,\tau)U_y^*(r_2,\tau)\rangle}{2},$$

$$\nu_2 = \frac{\langle U_x(r_1,\tau)U_y^*(r_2,\tau)\rangle - \langle U_y(r_1,\tau)U_x^*(r_2,\tau)\rangle}{2}, \tag{4}$$

$$\nu_3 = \mathrm{i}\frac{\langle U_x(r_1,\tau)U_y^*(r_2,\tau)\rangle - \langle U_y(r_1,\tau)U_x^*(r_2,\tau)\rangle}{2}.$$

These parameters are measured in sequence at different orientations of the polarisation filter, placed before the photodetector. The coefficient ν_1 is given by the difference of visibility values for the rotation angles 0° and 90° of a linear analyser transmission plane with respect to the plane of incidence, the coefficient ν_2 is the same for the rotation angles 45° and 135°, and ν_3 is the same for the rotation of the fast axis of a quarter-wave plate by the angles +45° (right-hand circular polarised wave) and –45° (left-hand circular polarised wave).

It can be shown that in the case of a steady-state field of the scattered laser radiation expression (3) for CDMP takes the form

$$V(r_1,r_2) = \frac{(U_x(r_1)U_x^*(r_2)+U_y(r_1)U_y^*(r_2))^2}{I(r_1)I(r_2)}. \tag{5}$$

The theoretical approach (1)–(5) was extended to the coordinate analysis of polarisation-inhomogeneous laser images of a human BT [25,26,32]. In [25] it is proposed to measure the real part of CDMP using a direct polarisation method for the points r_1, r_2 of the image of optically thin (the attenuation coefficient $\tau \le 0.1$) layers of the BT:

$$\operatorname{Re} V \equiv \tilde{V}(r_1, r_2) = \frac{\{U_x(r_1)U_x(r_2) - U_y(r_1)U_y(r_2)\cos[\varphi(r_1) - \varphi(r_2)]\}^2}{I(r_1)I(r_2)}, \quad (6)$$

where $\varphi(r_1)$ и $\varphi(r_2)$ are the phase shifts between the orthogonal components U_x, U_y of the amplitude at the points r_1, r_2. Using (6) a method of polarisation-correlation mapping [polarisation measurement of 2D distributions $\tilde{V}(x,y)$] of laser images of BTs is developed [26].

As a result of the studies [26, 33–37], the regions of variation in first- to fourth-order statistical moments of $\tilde{V}(x,y)$ distributions were determined for laser images of human connective tissue, which are urgent for the diagnostics of its oncologic status. However, such methods of analysing $\tilde{V}(x,y)$ do not account for the birefringence of protein fibrils as the main physical mechanism of formation of BT polarisation-inhomogeneous images [3, 11, 13, 18, 33, 34]. Therefore, the search for new diagnostic parameters that directly characterise the degree of coordination in optical axis orientations and birefringence at different points of the BT protein crystal network seem to be an urgent problem [3, 6, 7, 12, 14, 18, 24, 34, 35]. In analogy with [23] we will refer such a parameter as the complex degree of mutual anisotropy (CDMA).

The aim of the present work is to introduce and justify a method of polarisation-correlation mapping of birefringent networks of BTs for diagnostics of their physiological condition using the statistical analysis of the CDMA coordinate distributions.

2. Theoretical analysis of mechanisms, transforming laser radiation parameters in a network of birefringent optically uniaxial protein crystals

We consider the processes of interaction of laser radiation with a BT in the following model approximation:

(i) According to the classification by Cowin [36], morphologically all human tissues are divided into four basic types (connective, muscular, epithelial, and neural), each having a two-component amorphous-crystalline structure.

(ii) The crystalline component of the BT, or extracellular matrix, is formed by a network of coaxial cylindrical fibrils, consisting of a protein (collagen, elastin, myosin, etc.) [3, 6–8].

(iii) From an optical point of view, the protein fibrils possess the properties of uniaxial crystals with the birefringence index Δn (Fig. 1), whose anisotropy parameters $\rho(r)$ and $\delta(r)$ at each point r are described by the Jones operator [4, 35]

$$\{D\} = \begin{Vmatrix} d_{11}(r) & d_{12}(r) \\ d_{21}(r) & d_{22}(r) \end{Vmatrix} = \begin{Vmatrix} \theta^2 + \eta^2\exp(-i\delta(r)) & \theta\eta[1 - \exp(-i\delta(r))] \\ \theta\eta[1 - \exp(-i\delta(r))] & \eta^2 + \theta^2\exp(-i\delta(r)) \end{Vmatrix}. \quad (7)$$

Here, $\theta = \cos\rho(r)$; $\eta = \sin\rho(r)$; $\rho(r)$ is the angle (orientation) of the optical axis, determined by the direction of laying of the birefringent protein fibril with the transverse geometrical dimension $d(r)$; $\delta(r) = (2\pi/\lambda)\Delta n d(r)$ is the phase shift between the orthogonal components U_{0x} and U_{0y} of the amplitude U_0 of laser radiation with the wavelength λ at a point with the coordinate r.

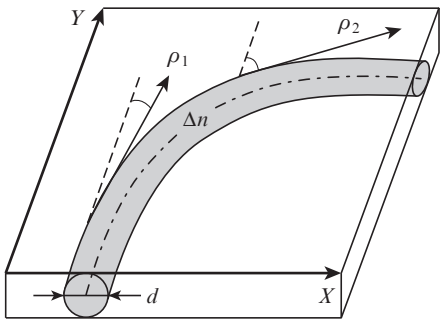

Figure 1. Birefringent (Δn) fibril with the cross-section diameter d; ρ_i are the directions of the optical axis in the plane of the BT layer.

Analytically the transformation of the amplitude and phase of the laser beam by the protein crystal of extracellular matrix of BT at a point with the coordinate r can be described by the equation

$$\begin{pmatrix} U_x(r) \\ U_y(r) \end{pmatrix} = \begin{Vmatrix} d_{11}(r) & d_{12}(r) \\ d_{21}(r) & d_{22}(r) \end{Vmatrix} \begin{pmatrix} U_{0x} \\ U_{0y}\exp(-i\delta_0) \end{pmatrix} = \begin{pmatrix} d_{11}(r)U_{0x} + d_{12}(r)U_{0y}\exp(-i\delta_0) \\ d_{21}(r)U_{0x} + d_{22}(r)U_{0y}\exp(-i\delta_0) \end{pmatrix} = \begin{pmatrix} d_{11}(r) + d_{12}(r)\tan\Omega_0\exp(-i\delta_0) \\ d_{21}(r) + d_{22}(r)\tan\Omega_0\exp(-i\delta_0) \end{pmatrix}. \quad (8)$$

Here δ_0 is the phase shift between the components U_{0x} and U_{0y}; $\tan\Omega_0 = U_{0y}/U_{0x}$.

The analysis of expressions (8) reveals the dependence of the orthogonal components $U_x(r)$, $U_y(r)$ of the complex amplitude on the rotation angle Ω_0 of the polarisation plane of the illuminating laser wave, or upon the angle of rotation γ of the BT layer itself with respect to the direction of irradiation. This circumstance impedes the implementation of the relative diagnostic analysis of CDMA of extracellular matrix in different BTs. The only exception is the case of irradiating the BT with a circularly polarised laser wave U_0:

$$U_0 = \begin{pmatrix} U_{0x} \\ U_{0y} \end{pmatrix} \equiv \frac{1}{\sqrt{2}}\begin{pmatrix} 1 \\ i \end{pmatrix}. \quad (9)$$

Keeping this in mind, to derive the analytic expression for CDMA $W(r_1, r_2)$ at the points r_1, r_2 of the extracellular matrix of a BT we make use of Eqns (5), (7), taking Eqns (8) and (9) into account:

$$W(r_1, r_2) = \{[d_{11}(r_1) + id_{12}(r_1)][d_{11}(r_2) + id_{12}(r_2)]^* + [d_{21}(r_1) + id_{22}(r_1)][d_{21}(r_2) + id_{22}(r_2)]^*\}^2 \big/ I(r_1)I(r_2), \quad (10)$$

where

$$I(r_1) = \{[d_{11}(r_1) + id_{12}(r_1)][d_{11}(r_1) + id_{12}(r_1)]^* + [d_{21}(r_1) + id_{22}(r_1)][d_{21}(r_1) + id_{22}(r_1)]^*\};$$
$$I(r_2) = \{[d_{11}(r_2) + id_{12}(r_2)][d_{11}(r_2) + id_{12}(r_2)]^* + [d_{21}(r_2) + id_{22}(r_2)][d_{21}(r_2) + id_{22}(r_2)]^*\}. \quad (11)$$

Extracting the real parts $\mathrm{Re}\, d_{ik}(r) \equiv \tilde{d}_{ik}(r)$ of the Jones matrix elements [Eqns (7)], we arrive at the expression for the real part of the CDMA $\mathrm{Re}\, W(r_1,r_2) \equiv \tilde{W}(r_1,r_2)$ of the BT layer extracellular matrix. To do so, we perform direct polarisation measurements:

$$\tilde{W}(r_1,r_2) = \{[\tilde{d}_{11}(r_1)\tilde{d}_{11}(r_2) - \tilde{d}_{12}(r_1)\tilde{d}_{12}(r_2)] + [\tilde{d}_{21}(r_1)\tilde{d}_{21}(r_2) - \tilde{d}_{22}(r_1)\tilde{d}_{22}(r_2)]\}^2 / I(r_1)I(r_2), \quad (12)$$

where

$$\tilde{d}_{11}(r) = \cos^2\rho(r) + \sin^2\rho(r)\cos\delta(r);$$
$$\tilde{d}_{12,21}(r) = \cos\rho(r)\sin\rho(r)(1 - \cos\delta(r)); \quad (13)$$
$$\tilde{d}_{22}(r) = \sin^2\rho(r) + \cos^2\rho(r)\cos\delta(r).$$

In Table 1 the basic characteristic values of CDMA $\tilde{W}(r_1,r_2)$ at arbitrary points r_1, r_2 of the BT layer extracellular matrix are summarised.

Table 1. Characteristic values of CDMA $\tilde{W}(r_1,r_2)$ of the BT layer extracellular matrix and CDMP $\tilde{V}(r_1,r_2)$ of its laser image.

Phase shifts at the points r_1 and r_2		CDMA	CDMP
$\delta(r_1) = \delta(r_2)$	$\delta(r_1) = \delta(r_2) = 0$	1.0	1.0
	$\delta(r_1) = \delta(r_2) = 0.5\pi$	1.0	1.0
	$\delta(r_1) = \delta(r_2) = \pi$	1.0	1.0
$\delta(r_1) = 0.5\pi + \delta(r_2)$	$\delta(r_1) = 0.5\pi$, $\delta(r_2) = 0$	0.5	0.5
	$\delta(r_1) = \pi$, $\delta(r_2) = 0.5\pi$	0.5	0.5
	$\delta(r_1) = 1.5\pi$, $\delta(r_2) = \pi$	0.5	0.5
$\delta(r_1) = \pi + \delta(r_2)$	$\delta(r_1) = \pi$, $\delta(r_2) = 0$	0	0
	$\delta(r_1) = 1.5\pi$, $\delta(r_2) = 0.5\pi$	0	0
	$\delta(r_1) = 2\pi$, $\delta(r_2) = \pi$	0	0

From the analysis of the presented data it follows that in the case of single scattering of laser radiation a one-to-one interconnection exists between the characteristic values of CDMA $\tilde{W}(r_1,r_2)$ of the BT layer and CDMP $\tilde{V}(r_1,r_2)$ of its laser image.

3. Optical scheme and technique of experimental measurement of 2D CDMA distributions of the extracellular matrix of a biological tissue

The experimental studies of the CDMA coordinate distributions were carried out in the classical polarimeter scheme, the basic units and elements of which are illustrated in Fig. 2.

The polarisation illuminator [quarter-wave plates (*3*,*5*) and polariser (*4*)] sequentially produced a set of probing laser beams, including the linearly polarised ones with the azimuthal angles $\alpha_0 = 0, +45°, 90°$, and the right-hand circularly polarised wave ($\delta_0 = 90°$). The corresponding polarisation images of the BT layer (*6*) produced by the microscope objective (*7*) were projected onto the plane of the light-sensitive area (600×800 pixels) of the digital camera (*10*), providing the measurement of structural elements in the interval 2–2000 μm. The polarisation analysis of the BT images was implemented with a system, including a quarter-wave plate (*8*) and polariser (*9*).

First, following the classical method, described in [6], the two-dimensional distribution of the real parts of the Jones matrix elements $\tilde{d}_{ik}(m \times n)$ of a histological section of BT (*6*) was measured. Then, by rotating the transmission plane of analyser (*9*) within the limits $\Theta = 0–180°$, the minimal $[I_{\min}(r_{jk})]$ and maximal $[I_{\max}(r_{jk})]$ level of the intensity was determined for each pixel (r_{jk}) of the CCD-camera (*10*)

$$\begin{pmatrix} r_{11} & \dots & r_{1m} \\ \dots & \dots & \dots \\ r_{n1} & \dots & r_{nm} \end{pmatrix}$$

being the coordinates of $m \times n$ pixels of this camera.

Following this technique, we obtained the arrays of extreme intensity values $I_{\min}(m \times n)$, $I_{\max}(m \times n)$ for the laser image of the histological section of BT (*6*) and the corresponding rotation angles $\Theta_{\min}(m \times n) \leftrightarrow I_{\min}(m \times n)$ of analyser (*9*). From these data the coordinate distributions of the polarisation azimuth $\alpha(m \times n)$ and ellipticity $\beta(m \times n)$ were calculated and the two-dimensional distributions of the phase shifts $\delta(m \times n)$ were determined using the following algorithms:

$$\alpha(r) = 0.5\pi - \Theta(r),$$
$$\beta(r) = \arctan\frac{I_{\min}(r)}{I_{\max}(r)}, \quad (14)$$
$$\delta(r) = \arctan\frac{\tan 2\beta(r)}{\tan\alpha(r)}.$$

The value of CDMA $\tilde{W}(r_1, r_2 = r_1 + \Delta r)$ for two points $(r_1, r_1 + \Delta r)$ of the protein crystal network, shifted by the interval Δr, was calculated using the algorithm (12), (13).

The coordinate distribution $\tilde{W}(x,y)$ of the extracellular matrix of the whole layer of the BT was determined by scanning the arrays $\tilde{d}_{ik}(m \times n)$ and $\delta(m \times n)$ in two mutually perpendicular directions ($x = 1, ..., m$, $y = 1, ..., n$) with the step $\Delta r =$ 1 pixel.

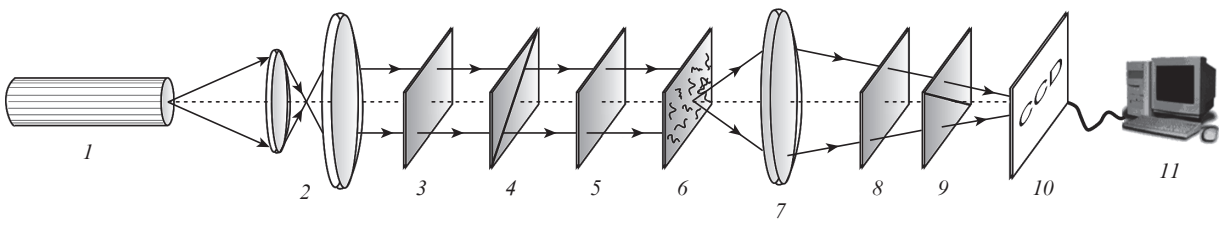

Figure 2. Optical scheme of the polarimeter for measuring the coordinate distributions of CDMA in the BT:
(*1*) He–Ne laser ($\lambda = 0.6328$ μm); (*2*) collimator; (*3*,*5*,*8*) quarter-wave plates; (*4*,*9*) polarisers; (*6*) histological section of the BT; (*7*) projection microscopic objective; (*10*) CCD-camera; (*11*) computer.

4. Experimental studies of 2D distributions of CDMA for the extracellular matrix of the BT in different physiological states

Note, that the structure of the anisotropic component of different BT types is rather complex and various [3, 6, 7, 12, 13, 18, 34–36]. Therefore, the statistical approach is appropriate, i.e., the study of relations between the statistical moments of first-to-fourth orders, which characterise the coordinate distributions $\tilde{W}(x,y)$ of the extracellular matrix of the BT with pathologically modified orientation-phase structure.

The histological sections of healthy and pathologically modified dermal skin layer (DSL) we used as objects of study. A specific structural feature of the extracellular matrix of a healthy DSL is the chaotic distribution of the directions $[\rho(n\times m)]$ of the protein crystal optical axes (Fig. 3). The extracellular matrix of pathologically modified DSL is characterised by a set of ordered 'neogenic' collagen fibrils with a high birefringence index [12].

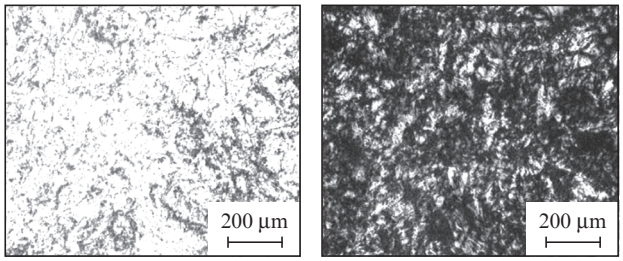

Figure 3. DSL image at parallel (a) and crossed (b) axes of the polariser and analyser.

Figure 4 shows a series of coordinate distributions for physiologically normal and pathologically modified DSL samples. The analysis of the obtained data shows that the coordinate distributions of CDMA (Figs 4a, d) are composed of local areas (domains $\tilde{W} \approx \text{const}$, Figs 4b, e) with the maximal variation interval $0{,}0 \le \tilde{W} \le 1{,}0$ (Figs 4c, f).

The obtained experimental data are in satisfactory correlation with the results of the proposed model analysis of the extracellular matrix structure using the CDMA. Thus, in the network of protein fibrils it is always possible to find points $(r, r + \Delta r)$, determining such relations between the anisotropy parameters r, δ (see Table 1), to which the extreme values of the CDMA correspond

$$\tilde{W}(r, r + \Delta r) = \begin{cases} 0{,}0 \\ 1{,}0. \end{cases}$$

The specific features of the morphological structure of the BT extracellular matrix manifest themselves also in different probabilities of particular values of $\tilde{W}(x,y)$. For a randomly oriented network of collagen fibrils in the DSL (Figs 4a, b) the histograms of the layer represent sufficiently equiprobable distributions (Fig. 4c).

Pathological modifications of the DSL collagen structures manifest themselves (Figs 4d, e) in a certain localisation of the random quantity distributions of CDMA (Fig. 4f) in the domain of extreme values ($\tilde{W} = 0.4$–0.6).

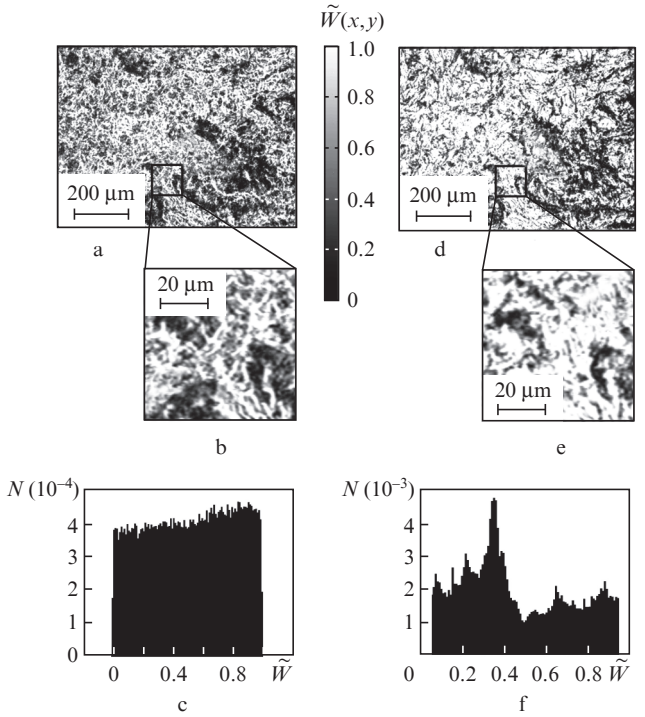

Figure 4. Coordinate distributions 600×800 pixels (a, d), 50×50 pixels (b, e), and histograms (c, f) of $\tilde{W}(x,y)$ values in physiologically normal (a–c) and pathologically modified (d–f) histological sections of the DSL.

The next step was to perform a comparative study of the diagnostic efficiency of CDMP ($\tilde{V}(x,y)$) and CDMA ($\tilde{W}(x,y)$) methods under the conditions of single and multiple scattering of laser radiations by the BT layers in different physiological status.

5. Comparative statistical analysis of 2D CDMA distributions for the extracellular matrix of dermal skin layer and CDMP of their laser images

To determine the range of variation for the statistical moments, characterising the coordinate distributions $\tilde{W}(x,y)$ and $\tilde{V}(x,y)$, the histological sections of the DSL were divided into two groups, consisting of 20 normal and 19 pathologically modified samples.

The statistical first-to-fourth-order moments for the distributions

$$Q = \begin{cases} \tilde{V} \\ \tilde{W} \end{cases}$$

were calculated using the MATLAB software employing the following algorithms [11]:

$$M_1 = \frac{1}{N}\sum_{i=1}^{N} |Q_i|, \quad M_2 = \sqrt{\frac{1}{N}\sum_{i=1}^{N} Q_i^2}, \tag{15}$$

$$M_3 = \frac{1}{M_2^3}\frac{1}{N}\sum_{i=1}^{N} Q_i^3, \quad M_4 = \frac{1}{M_2^2}\frac{1}{N}\sum_{i=1}^{N} Q_i^4,$$

Table 2. Statistical first- to fourth-order moments for the distributions of CDMA and CDMP in optically thin ($\tau = 0.09$) and optically thick ($\tau = 0.75$) (in parentheses) layers of physiologically normal and pathologically modified samples of the DSL.

DSL	Method of measurement	M_1	M_2	M_3	M_4
Normal	CDMA	0.38±0.04 (0.45±0.051)	0.10±0.02 (0.16±0.014)	9.4±0.87 (8.65±0.83)	99.5±9.63 (43.3±4.88)
(20 samples)	CDMP	0.27±0.03 (0.37±0.041)	0.07±0.008 (0.27±0.033)	14.7±1.16 (0.77±0.082)	76.9±6.98 (1.13±0.15)
Pathological	CDMA	0.33±0.04 (0.63±0.057)	0.085±0.009 (0.18±0.021)	21.7±1.96 (12.1±1.18)	36.9±4.08 (29.7±3.07)
(19 samples)	CDMP	0.31±0.03 (0.41±0.039)	0.063±0.008 (0.23±0.025)	19.4±1.78 (1.08±0.09)	42.6±4.17 (0.86±0.09)

where $N = m \times n$ is the number of pixels of the light-sensitive matrix of the digital camera.

Table 2 presents the results of calculations of the mean value (M_1), variance (M_2), skewness (M_3) and kurtosis (M_4) for the distributions of CDMA $\tilde{W}(x,y)$ of dermal skin layers with various optical thickness and CDMP $\tilde{V}(x,y)$ of their laser images.

From the obtained data on the coordinate distributions of CDMA in optically thin layers of BT it follows that

(i) The mean and variance of the coordinate distributions $\tilde{W}(x,y)$ in optically thin layers differ insignificantly between the normal and pathologically modified DSLs, namely, by the factors from 1.3 (M_1) to 1.5 (M_2). For 2D distributions $\tilde{V}(x,y)$ of the CDMP of the corresponding laser images there is practically no difference in the values of their statistical moments of the first and second order.

(ii) The values of the skewness of the coordinate distributions $\tilde{W}(x,y)$ of the samples of BT under study differ by 2.1 times and those of kurtosis by 3.2 times. For the CDMP distributions $\tilde{V}(x,y)$ the values of the third and the fourth statistical moments change as follows: 1.3 times for M_3 and 1.8 times for M_4. Moreover, with growing multiplicity of scattering, due to the cross-interference of coherent waves $U_j(r)$ with different polarisations, the azimuth and ellipticity distributions of the BT object field polarisation are changed. As a result, the unambiguity of the mutual relation between the parameters of $\tilde{W}(x,y)$ and $\tilde{V}(x,y)$ is 'destroyed'.

(iii) Statistical moments of higher orders may be used as diagnostically valuable parameters of the physiological conditions of thick BTs. The values of skewness of the coordinate distributions $\tilde{W}(x,y)$ for normal and pathologically modified DSLs differ by 1.4 times, and those of kurtosis M_4 differ by 1.45 times.

(iv) The statistical moments of the third and fourth order for the two-dimensional distributions $\tilde{V}(x,y)$ of CDMP of the object field of optically tick layers of BT weakly depend on their physiological status and are an order of magnitude smaller than the skewness and kurtosis of CDMP $\tilde{W}(x,y)$.

6. Conclusions

To estimate the degree of coordination of parameters, characterising the network of optically uniaxial birefringent protein fibrils in biological tissues we introduce a new parameter, referred as the complex degree of mutual anisotropy. A method for polarisation measurement of coordinate distributions of the complex degree of mutual anisotropy in biological tissues is developed. It is shown that the statistical approach to the analysis of the distributions $\tilde{W}(x,y)$ in biological tissues, whose optical thicknesses lie within the interval $\tau = 0.09 - 0.75$, which corresponds to the conditions of both single and multiple scattering, is more sensitive and efficient as a tool for the differentiation of their physiological condition, compared to the studies of the complex degree of mutual polarisation of the corresponding laser images.

References

1. Patterson M.S., Andersson-Engels S., Wilson Brian C., Osei E.K. *Appl. Opt.*, **34**, 22, (1995).
2. Alfano R.R., Fujimoto J.G. (Eds). *Advances in Optical Imaging and Photon Migration* (Topics in Optics and Photonics Series) (Washington: Opt. Soc. of America, 1996) Vol. 2.
3. Ushenko A.G., Pishak V.P., in *Handbook of Coherent-Domain Optical Methods: Biomedical Diagnostics, Environmental and Material Science* (Boston: Kluwer Acad. Publ., 2004) Vol. 1, pp. 93–138.
4. Gori F., Santarsiero M., Vicalvi S., Borghi R., Guattari G. *Pure Appl. Opt.*, **7**, 941 (1998).
5. Wolf E. *Phys. Lett. A.*, **312**, 263, (2003).
6. Angelsky O.V., Ushenko A.G., Ushenko Yu.A., Pishak V.P., in *Optical Correlation Techniques and Applications* (Washington: Soc. Photo-Opt. Instrum. Eng., 2007) pp. 213–266.
7. Angelsky O.V., Ushenko A.G., Ushenko Yu.A., Pishak V.P., Peresunko A.P., in *Diagnostics of the Structure and Physiological State of Birefringent Biological Tissues. Handbook of Photonics for Biomedical Science* (New York: CRC Press, 2010) pp. 21–67.
8. Ushenko A.G. *Opt. Eng.*, **34** (4), 1088 (1995).
9. Ushenko A.G., Ermolenko S.B., Burkovets D.N., Ushenko Yu.A. *Opt. Spektrosk.*, **87** (3), 434 (1999).
10. Angelsky O.V., Ushenko A.G., Arkhelyuk A.D., Ermolenko S.B., Burkovets D.N., Ushenko Yu.A. *Opt. Spektrosk.*, **89** (6), 973 (2000).
11. Ushenko A.G. *Stokes-correlometry of Biotissues*, **10** (5), 1286 (2000).
12. Ushenko A.G. *Laser Phys.*, **10** (5), 1143 (2000).
13. Ushenko A.G., Burkovets D.N., Ushenko Y.A. *Laser Phys.*, **11** (5), 624 (2001).
14. Angelsky O.V., Ushenko A.G., Burkovets D.N., Ushenko Yu.A. *Opt. Spektrosk.*, **90** (3), 458 (2001).
15. Ushenko A.G. *Opt. Spektrosk.*, **91** (2), 313 (2001).
16. Ushenko A.G. *Opt. Spektrosk.*, **91** (6), 937 (2001).
17. Ushenko A.G. *Opt. Spektrosk.*, **91** (6), 932 (2001).
18. Angelsky O.V., Ushenko A.G., Ushenko Yu.A. *J. Holography Speckle*, **2** (2), 72 (2002).
19. Angelsky O., Ushenko A., Burkovets D., Pishak V., Ushenko Yu., Pishak O. *Laser Phys.*, **10** (5), 1136 (2000).
20. Ushenko A.G. *Opt. Spektrosk.*, **92** (2), 227 (2002).
21. Angelsky O.B., Ushenko A.G., Ushenko Yu.A. *J. Holography Speckle*, **2** (1), 26 (2005).
22. Ellis J., Dogariu A., Ponomarenko S., Wolf E. *Opt. Lett.*, **29**, 1536 (2004).
23. Ellis J., Dogariu A. *Opt. Lett.*, **29**, 536 (2004).
24. Angelsky O.V., Tomka Yu.Ya., Ushenko A.G., Ushenko Yu.A. *J. Phys. D: Appl. Phys.*, **38** (23), 4227 (2005).
25. Angelsky O.V., Ushenko A.G., Ushenko Ye.G. *J. Biomed. Opt.*, **10** (6), ID 060502 (2005).
26. Angelsky O.V., Ushenko A.G., Ushenko Ye.G. *Phys. Med. Biol.*, **50**, 4811 (2005).
27. Tervo J., Setala T., Friberg A. *Opt. Express*, **11**, 1137, (2003).
28. Movilla J.M., Piquero G., Martínez-Herrero R., Mejías P.M. *Opt. Commun.*, **149**, 230 (1998).
29. Mujat C., Dogariu A. *J. Opt. Soc. Am. A.*, **21** (6), 1000 (2004).
30. Gori F. *Opt. Lett.*, **23**, 241 (1998).

31. Mujat M., Dogariu A. *Opt. Lett.*, **28**, 2153 (2003).
32. Angelsky O.V., Ushenko A.G., Angelska A.O. *Ukrainian J. Phys. Opt.*, **8** (2), 105 (2002).
33. Ushenko A.G., Burkovets D.N., Ushenko Yu.A. *Opt. Spektrosk.*, **93** (3), 449 (2002).
34. Angelsky O.V., Ushenko A.G., Burkovets D.N., Ushenko Yu.A. *J. Biomed. Opt.*, **10** (1), ID 014010 (2005).
35. Angelsky O.V., Ushenko A.G., Burkovets D.N., Ushenko Yu.A. *Optica Applicata*, **32** (4), 591 (2002).
36. Cowin S.C. *J. Biomed. Eng.*, **122**, 553 (2000).
37. Olar E.I., Ushenko A.G., Ushenko Yu.A. *Laser Phys.*, **14**, 1012 (2004).